# Theory of the $\alpha$-$\gamma$ phase transition in Ce

J. Lægsgaard and A. Svane
*Institute of Physics and Astronomy, University of Aarhus, DK-8000 Aarhus C, Denmark*
(Received 8 September 1998)

The Kondo volume collapse model of the isostructural $\alpha$-$\gamma$ phase transition in elemental cerium is investigated by a combination of the self-interaction-corrected local-density approximation (SIC-LDA) and the Anderson impurity model. The zero-temperature uncorrelated total-energy function as well as the model hybridization parameters are calculated with the SIC-LDA approach, while temperature and correlation effects are calculated within the impurity model, using an extension of the noncrossing approximation. It is found that the phase transition may be quantitatively well described with this approach, provided a rescaling of the hybridization parameters is invoked. The influence of Ce $f^2$ configurations on the accuracy of the calculations is discussed. [S0163-1829(99)03105-7]

## I. INTRODUCTION

One of the most fascinating properties of elemental Ce is the occurrence of the isostructural $\alpha$-$\gamma$ phase transition.[1] At low temperatures and ambient pressure, the equilibrium phase of Ce is the $\alpha$ phase, which has the fcc crystal structure and relatively low volume. At higher temperatures, the $\gamma$ phase, likewise fcc, but with a significantly larger volume, becomes stable. When pressure is increased, the crystal collapses back into the $\alpha$ phase in a first-order phase transition. At room temperature, the phase transition happens at a pressure of $\sim 7$ kbar, and the change in volume is 14.8%. The $\alpha$-$\gamma$ transition is unique among the elements in that it terminates in a critical point.[1]

Although it is generally accepted that the $\alpha$-$\gamma$ transition is connected to the behavior of the Ce $4f$ electron, several theoretical models have been put forward, invoking different physical effects. In the promotional model[2] it is assumed that the *f* level becomes depopulated upon compression, but this is hard to reconcile with cohesive properties,[3] positron annihilation,[4] and photoemission experiments,[5] which do not indicate major changes in the *f*-state occupation numbers across the phase boundary. Furthermore, a binding energy of the *f* level of the order of 0.1 eV or less would be necessary to account for the phase diagram within this model, which would imply that the width of the *f* band must be much narrower to speak meaningfully of the *f*-level position being above or below the Fermi level. However, both these requirements are at variance with spectroscopic experiments, and are not supported by band-structure calculations either.[6–9]

The Mott transition model of Johansson[3] assumes that the $\alpha$ phase of Ce is well described as an ordinary band state, while the $\gamma$ phase consists of localized $4f$ electrons. In a simple Hubbard-model[10] or Anderson-model[11] picture, the hopping terms in the Hamiltonian favor the formation of extended (bandlike) states, while the strong Coulomb repulsions between electrons sitting in the same $4f$ multiplet favor localization, which suppresses charge fluctuations on the different ions in the lattice. As the crystal is compressed, the hopping integrals increase in value, and eventually the bandlike states should be favored. In this picture, the $\alpha$-$\gamma$ transition is therefore similar to the Mott-Hubbard metal-insulator transition,[10] although both phases of Ce are metallic because the $spd$ electrons do not localize.

In the Kondo volume collapse (KVC) model[12,13] both the $\alpha$ and $\gamma$ phases of cerium are characterized by having highly correlated, localized *f* electrons. The difference is in the degree of localization: While the picture of the $\gamma$ phase that emerges is that of a quite localized *f* electron, with a deviation from integral occupancy of only a few %, the $\alpha$ phase tends towards the mixed-valent regime with an *f* occupation of only 0.86,[14] and the ground state is thus a complicated entanglement of *f* and $spd$ electrons. The latter phase clearly has the largest bonding energy, but entropy favors the phase with localized electrons, which explains why the $\gamma$ phase becomes stable at elevated temperatures and low pressures. The KVC model is supported by results from photoemission spectroscopy of the $\alpha$ phase,[5] which are more easily reconciled with the Anderson impurity model than with a bandlike picture.[14] The description of the $\alpha$ phase as either a single Slater determinant, or an entangled many-body state, constitutes the main difference between the Mott transition and KVC models.

The KVC model has been analyzed in detail by Liu and co-workers.[14] By fitting the parameters of the Anderson impurity Hamiltonian to spectroscopic information, and combining the impurity calculations with structural data for La and Pr, these authors were able to account for all qualitative features of the transition, and also to obtain reasonable quantitative predictions for the transition pressure as a function of temperature. The magnitude of the volume collapse was, however, underestimated by $\sim 40\%$.

The Mott transition model has recently been considered by several groups using *ab initio* electronic structure calculations.[15–17] In these works, the $\alpha$ phase is described by the conventional local-density approximation (LDA) to density-functional theory (DFT), with the *f* electrons participating in the band formation, while slightly different descriptions of the $\gamma$ phase are invoked. In Ref. 15 one *f* electron on each Ce atom is fixed in the core, while the remaining three valence electrons form ordinary LDA bands. An energy shift is introduced to align tetravalent and trivalent total energies.

 

In Ref. 16 one $f$ electron per Ce atom is localized by the self-interaction-corrected local-density approximation[18] (SIC-LDA) by which the tetravalent and trivalent phases constitute competing local minima of the same total energy functional. Consequently, the energy separation of the two phases may be calculated by the SIC-LDA approach, which in addition imposes strict orthogonality between the localized $f$ electrons and the normal valence electrons. By imagining the Ce crystal at finite temperatures to consist of an alloylike mixture of the trivalent and tetravalent Ce atoms, a description of the thermodynamics may be obtained by both approaches. In Ref. 17 it is assumed that the $\gamma$ phase may also be described as a conventional spin-polarized band state within LDA. The phase transition is then caused by a large entropy contribution from the band electrons. These works show that the Mott transition description, like the KVC model, captures the qualitative aspects of the $\alpha$-$\gamma$ phase transition of cerium, maybe with somewhat larger quantitative errors. On the other hand, the calculations are done without any adjustable parameters (one energy alignment parameter enters in Ref. 15). The LDA has had a tremendous success in the quantitative description of solids,[19,20] but the rare earths are extreme cases, for which the validity of the approximation is dubious. In particular, the simple picture of localized versus Bloch-like $f$ electrons cannot account for the results of spectroscopic experiments, so at least in the excited states of the system, some nontrivial correlations must be present. It is difficult to explain why these effects should not be present in the ground state as well. Also, there is no experimental evidence in favor of the alloy model used in Refs. 15 and 16.

In the present work we investigate the possibility of combining the KVC picture in the impurity model description of Liu and Allen with the SIC-LDA method used by Svane, to shed light on the possible connections between the two models and to reduce the number of adjustable parameters in the KVC calculation. In Sec. II a short review of previous work is given, serving as both motivation and formal preparation for the following sections. In Sec. III the formal theory of the present work will be presented, while Sec. IV presents the numerical results and Sec. V contains the conclusions and outlooks.

## II. REVIEW OF PREVIOUS WORK

In the KVC calculation performed by Allen and Liu,[14] it was assumed that the free energy of the Ce crystal could be split into two parts: A ''normal'' part $E_N$, arising from the non-$f$ electrons, and an $f$-electron part $E_f$, which was assumed to be equal, in an $N$-atom crystal, to the sum of free energies of $N$-independent impurity multiplets. $E_f$ was further subdivided into zero-temperature and finite-temperature contributions, while the temperature dependence of $E_N$ was assumed to be negligible. The zero-temperature part of $E_f$ was determined as the ground-state energy (that is, the difference between the ground-state energy with and without $f$-$spd$ interactions) of an Anderson impurity model as calculated by the method of Gunnarsson and Schönhammer.[21] In this method, the problem is treated within a finite basis set, consisting of eigenstates of the unhybridized problem. Allen and Liu used an expansion incorporating $f^0$, $f^1$, and $f^2$ configurations. The hybridization function was calculated from the $4f$-projected density of states (DOS) obtained in an LDA calculation for Ce, and subsequently rescaled (by an energy-independent parameter) to match photoemission data for the $\alpha$ and $\gamma$ phases. Slightly different rescaling parameters were necessary in the two phases. Afterwards, another rescaling (with the same factor for both phases) was done to match the measured values for the static magnetic susceptibility. Thus, the model cannot simultaneously account for the two sets of experimental data, possibly due to inaccuracies in the shape of the LDA hybridization function. The hybridization was taken to be identical for all states in the $4f$ multiplet, but a spin-orbit splitting of 0.28 eV was introduced between the $j=\frac{5}{2}$ and $j=\frac{7}{2}$ multiplets. At intermediate volumes, the hybridization function was found by linear interpolation between the functions calculated for the $\alpha$ and $\gamma$ volumes. The $f$-level position and $U$ value were also determined from fits to spectroscopy results. The finite-temperature contribution to the $f$-electron free energy $E_f$ was estimated from the Bethe-ansatz solution of the Kondo Hamiltonian with an impurity degeneracy of 6, corresponding to the degeneracy of the $j=\frac{5}{2}$ multiplet that carries most of the $f$ occupation.

The estimation of $E_N$ is not a trivial matter, since no phase of Ce is found in which the $f$ electrons do not contribute to the cohesion at all. Indeed, the Gunnarsson-Schönhammer calculations performed by Allen and Liu showed that *both* the $\alpha$ and $\gamma$ phases have large $f$-related contributions to the cohesive energy, mainly arising from $f^1$-$f^2$ fluctuations. Allen and Liu determined $E_N$ from the average values of equlibium volume and bulk modulus for La and Pr, which are neighbors of Ce in the Periodic Table and do not show anomalous behavior. Since the $f$ states also contribute to the cohesion in these compounds, $E_N$ must be determined by

$$E_N(v)=E^{La,Pr}(v)-E_f^{La,Pr}(v), \tag{1}$$

where $E^{La,Pr}(v)$ is a parabolic energy vs volume curve, obtained from the averages of La and Pr volumes and bulk moduli, while $E_f^{La,Pr}(v)$ is the average of the $f$ contribution to the total energy in the two compounds, as calculated in the Gunnarsson-Schönhammer formalism (again with parameters matched to various experimental data).

The physical picture emerging from the KVC calculation is roughly the following: The energy curve $E_N(v)$, which may be taken as a rough measure of the Ce total energy in the absence of $f^0$-$f^1$ fluctuations, has a minimum at a volume slightly larger than the $\gamma$-phase volume. The hybridization energy gained from $f^0$-$f^1$ hopping pulls the true total-energy minimum downwards to a value around the $\alpha$-phase volume, which is therefore the stable crystal volume at zero temperature. Actually, the $\alpha$-phase volume is somewhat overestimated in the calculation. In the $\alpha$ phase there is a relatively large energy separation between the ground state of the Anderson model, with its entanglement of the $f^0$ and $f^1$ configurations, and the excited states consisting essentially of a free localized $f$ electron, while at higher volumes, the energy separation is much smaller. Since the ground state is a singlet state, while there are six possible states for a localized electron, entropic contributions will favor the higher volumes when the temperature is large enough to break the ground-state singlet. These effects together bring about the phase

transition. Careful inclusion of the (large) hybridization energy from the $f^1$-$f^2$ fluctuations is important to obtain a reasonable quantitative description of the system, but the variation of this energy with volume does not show the exponential behavior characteristic of the $f^0$-$f^1$ hybridization.

The Mott transition calculation by Svane[16] assumes that the total energy of Ce at zero temperature can be described by DFT using the SIC-LDA approach.[18] The SIC-LDA total-energy functional may have several local minima, composed either entirely of Bloch wave functions, or of a combination of Bloch functions and localized orbitals. In Ce, it turns out that there are two minima of the total energy as a function of volume. In one minimum, at low volume, all electrons reside in orbitals with Bloch symmetry, while in the other minimum, at higher volume, a single electron at each site occupies a localized state that is of almost ($\sim$99%) pure $4f$ character. The localized electron does not contribute to the bonding, so in the first minimum Ce is tetravalent, while in the second minimum Ce is trivalent. Since the symmetry of the electronic states must be chosen from the outset (a set of Bloch states will, for instance, not evolve into non-Bloch states because they generate a translationally invariant potential), two distinct energy vs volume curves can be constructed for the two symmetries.[16] The minima occur at almost identical energies, the difference being $\sim 0.1$ mRy in favor of the low-volume phase, which is interpreted as the $\alpha$ phase. Due to the small difference in energy a negative pressure of only $-1$ kbar would be sufficient to affect a transition to the high-volume ($\gamma$-) phase. Extrapolating the experimental transition line to zero temperature, a transition ''pressure'' of $-7$ kbar is reached, so the result does not appear unreasonable. It should be emphasized, that the near degeneracy of the two energy minima may be coincidential. The calculations were performed within the atomic-spheres approximation (ASA) without inclusion of spin-orbit coupling, and the errors arising from these approximations are most probably larger than the difference in the minimum energies.

To extend the model to finite temperatures, Svane (similarly to Ref. 15) assumed that the entropy of the crystal is given as that of a mixture of tetravalent ($\alpha$-like) and trivalent ($\gamma$-like) atoms:

$$S = xS_\alpha + (1-x)S_\gamma + S_{mix}. \tag{2}$$

Here, $x$ denotes the fraction of $\alpha$-like ions. It is assumed that $S_\alpha = 0$, while $S_\gamma = k_B \ln 6$, corresponding to the sixfold degeneracy of the $j=\frac{5}{2}$ multiplet of the Ce $4f$ states. At most temperatures the inclusion of the $S_\gamma$ term is the decisive modification compared to the zero-temperature case. Only at high temperatures, close to the upper critical point of the phase transition, does the mixing entropy $S_{mix}$ become important. With this simple form for the entropy, the phase diagram as a function of temperature can be calculated. This calculation gives a critical point at a pressure of $p_c = 47$ kbar and temperature of $T_c = 1300$ K.[22] Experimentally, the critical coordinates are $(p_c, T_c) = (20$ kbar, 600 K$)$.[1] The volume collapse at room temperature is calculated to be 24%, significantly larger than the 14.8% observed experimentally. The volume of the $\gamma$ phase at the phase boundary is well described by the theory, while the volume of the $\alpha$ phase is severely underestimated. In conclusion, the calculation gives a good qualitative description of the phase transition, but the quantitative predictions are poor, compared to the work of Allen and Liu, which is perhaps to be expected, since the model does not contain adjustable parameters.

It is interesting to compare the physical content of the two theories outlined above. In the KVC model, the *f* bonding in the Anderson impurity model is characterized by a large contribution from $f^1$-$f^2$ fluctuations, which has relatively slow volume variation, and a smaller contribution from $f^0$-$f^1$ coupling, which varies much more rapidly with volume. The competition between this energy gain, at low volumes, and the gain in entropy at higher volumes brings about the phase transition. In the SIC-LDA picture, the *f*-occupation number is fluctuating ''freely'' in the $\alpha$ phase, i.e., in a manner characteristic of uncorrelated states, while in the $\gamma$ phase, one electron is frozen in the localized SIC state, which is essentially a local *f* state. Therefore, the $f^0$ configuration is excluded from occupation in the $\gamma$ phase. The normal conduction-band states are still allowed to hop into the *f* states orthogonal to the localized state, so higher configurations are also occupied in this case. In fact, the total *f* occupation is calculated to be around 1.3 in both the $\alpha$ and the $\gamma$ phases, which indicates that configurations with more than one *f* electron have a considerable weight. The energy difference between the LDA and SIC-LDA ground states is therefore given by the $f^0$-$f^1$ hybridization energy, and the SIC calculation may be viewed as a simple ''on/off'' approximation to the rapid volume variation of this term in the Anderson model. Thus, in a certain sense, the two models appear very similar, since the finite-temperature extension of the SIC-LDA calculation contains essentially the same entropic effects as the KVC calculation. The difference is in the description of the $f^0$-$f^1$ coupling in the $\alpha$ phase as either uncorrelated hopping or Kondo entanglement. In the $\gamma$ phase, the $f^0$ configuration has little weight in the KVC calculation, so the difference between the two approaches here is probably not very significant. Furthermore, the description of the $f^1$-$f^2$ coupling is very different in the two approaches in both the $\alpha$ and the $\gamma$ phases. This is evidenced by the significant difference in occupation numbers: While the LDA and SIC-LDA calculations find $n_f \sim 1.3$, the KVC model finds $n_f < 1$ for both phases.

To distinguish the two models from each other, we should therefore focus attention on the description of the $\alpha$ phase, and on the way in which the $f^1$-$f^2$ coupling is treated. With respect to the $\alpha$ phase, a closer look at the results of Svane reveals that most of the quantitative errors in the description arise from a severe underestimation of the $\alpha$-phase volume by the LDA calculation.[16] Indeed, a rigid shift of the LDA total-energy curve towards larger volumes before doing the thermodynamic calculation brought the coordinates of the critical point to an agreement, within errors, with the experimental value. One may speculate that the ''uncorrelated'' $f^0$-$f^1$ hybridization in the LDA calculation overestimates the cohesive contribution from these fluctuations and that a Kondo-like picture is more appropriate. On the other hand, the theoretical description of the $\alpha$-phase volume within DFT is significantly improved with the generalized gradient approximation (GGA).[23,24,17]

With the description of the $\gamma$ phase approximately correct

in both the KVC and SIC-LDA calculations, one could worry about the difference in *f*-occupation numbers (or, equivalently, in the couplings to higher configurations). From the KVC calculation of Ref. 14 it is not easy to judge how decisive the treatment of these couplings is, since the difference between $f^1$-$f^2$ hybridization energies (this energy calculated for Ce minus the average of this energy for La and Pr) is added to a parabolic ''normal'' contribution with a bulk modulus taken from experiments. Hence, one may to a certain extent expect cancellations of errors. In the case of the SIC-LDA calculation, where there are no adjustable parameters, it is easier to see that a drastic modification of this hybridization energy would perturb the results strongly. In the following we will estimate the $f^1$-$f^2$ hybridization energy from the band-structure calculations, and compare to the energies obtained in the KVC model.

In the following sections we will incorporate band theory into the KVC model. From the above discussion, two possibilities emerge, which will both be considered: In approach A, we start from a band calculation of a pure $f^1$ configuration, in which the *f* electrons do not contribute to the bonding at all. This is realized either by an LDA calculation in which one $4f$ orbital per Ce atom is occupied in a core state, or by a SIC-LDA calculation in which the Bloch states are expanded in $spd$ orbitals only. To the total energy evaluated in this calculation is then added a free-energy contribution from an impurity-model calculation taking all possible (in practice, all $f^0$, $f^1$, and $f^2$) configurations into account. In approach B, we start from a similar SIC-LDA calculation, however with the Bloch states expanded also in $4f$ orbitals. To the total energy of this calculation we add the impurity-model estimate of the $f^0$-$f^1$ hybridization free-energy contribution. The difference between the two approaches is the description of the couplings to multiply occupied *f* configurations.

## III. FORMAL THEORY

The total Helmholtz free energy per Ce ion is assumed to be given as

$$F(T,v)=E_0(v)+F_{imp}(T,v). \tag{3}$$

Here, $E_0$ is the zero temperature total energy from one of the DFT calculations mentioned above, and $F_{imp}$ is the hybridization contribution to the free energy of the impurity model. Thus all temperature variation of the free energy enters through the second term. The vibrational free energy and the entropy of the normal conduction electrons are not considered here. Both of these terms are small. In contrast to Ref. 17 the SIC-LDA does not lead to a large density of states at the Fermi level.

In the SIC-LDA approximation[18] one subtracts from the LDA total-energy functional[19] the self-Coulomb and self-exchange-correlation energy for each occupied electron state:

$$E_0(v)\equiv E^{SIC}[\{\psi_\alpha\}]=\sum_\alpha \langle\psi_\alpha|-\Delta|\psi_\alpha\rangle+U[n]+E_{xc}^{LDA}[\bar{n}] + V_{ext}[n]-\sum_\alpha \{U[n_\alpha]+E_{xc}^{LDA}[\bar{n}_\alpha]\}. \tag{4}$$

Here, $\alpha$ enumerates the occupied electron states. $\bar{n}$ is the total spin density of the system, $\bar{n}(\mathbf{r})=[n^\uparrow(\mathbf{r}),n^\downarrow(\mathbf{r})]$, $n(\mathbf{r})=n^\uparrow(\mathbf{r})+n^\downarrow(\mathbf{r})$, and $\bar{n}_\alpha$ is the spin density of the $\alpha$th state. $E^{SIC}$ is written as a functional of the set of occupied wave functions $\psi_\alpha$. It may be shown that $E^{SIC}$ is in fact a functional of the total spin density alone, $E^{SIC}=E^{SIC}[\bar{n}]$.[18,25] $U[n]$ and $E_{xc}^{LDA}[\bar{n}]$ are the Coulomb and the exchange-correlation energies of the electron gas, respectively, while $V_{ext}[n]$ denotes the interaction energy with the lattice of ions.

The last term in Eq. (4) constitutes the self-interaction correction, where for each occupied orbital the Coulomb and exchange-correlation energies of the corresponding spin density $\bar{n}_\alpha$ is subtracted. If the self-interaction is omitted we would have the LDA energy functional $E^{LDA}$. Since $E^{LDA}$ erroneously includes the self-interaction of each occupied orbital it is natural to correct for this, which is the motivation for considering the functional $E^{SIC}$.[18] The self-interaction vanishes identically for extended states, but is finite for spatially confined states. For well-localized states, like the $4f$ states of Ce, it is a negative energy contribution. The self-interaction correction may therefore also be viewed as an energy gained by localization, which counteracts the loss in band formation energy. The implementation of the minimization of the $E^{SIC}$ functional using the *ab initio* tight-binding linear muffin-tin orbital (LMTO) method[26–28] is described in detail in Ref. 16.

The second term in Eq. (3) may be written

$$F_{imp}(T,v)=-k_BT\ln Z_f, \tag{5}$$

where the partition function $Z_f$ of the *f* electrons due to the interactions with the normal conduction electrons will be assumed to be described by the Anderson impurity model:[11]

$$\hat{H}=\sum_{n\mathbf{k}} \varepsilon_{n\mathbf{k}}\hat{c}^\dagger_{n\mathbf{k}}\hat{c}_{n\mathbf{k}}+\sum_\nu \varepsilon_\nu\hat{n}_\nu+\frac{U}{2}\sum_{\nu\neq\nu'}\hat{n}_\nu\hat{n}_{\nu'} + \sum_{n\mathbf{k}\nu}(V_\nu^{n\mathbf{k}}\hat{f}^\dagger_\nu\hat{c}_{n\mathbf{k}}+\text{H.c.}) \tag{6}$$

The operators $\hat{f}$ and $\hat{c}$ are destruction operators for *f* and other electrons, respectively. $\hat{n}_\nu$ is the number operator for a particular orbital in the *f* multiplet (indexed by $\nu$). The orbital dependence of *f* energies originates from spin-orbit and possibly crystal-field splitting. We have chosen to ignore a possible orbital dependence of the *U* parameters, although the inclusion hereof is not a serious problem.

Assuming that *U* is the dominant energy scale in the problem, it is reasonable to expand the solution in eigenstates of the impurity Hamiltonian without the *f*-*c* hybridization term, i.e., states with fixed *f* and band occupation numbers. This approach is the basis of the Gunnarsson-Schönhammer approach[21] and the noncrossing approximation (NCA),[29] both widely used in the analysis of photoemission in Ce and Ce compounds. In the present work $Z_f$ will be evaluated in the generalized noncrossing approximation (NCA),[30,31] according to which

$$Z_f=\int_{-\infty}^{\infty}d\omega e^{-\beta\omega}\left[\rho^{(0)}(\omega)+\sum_{\nu}\rho_{\nu}^{(1)}(\omega)+\frac{1}{2}\sum_{\nu\nu'}\rho_{\nu\nu'}^{(2)}(\omega)\right], \tag{7}$$

when $f^2$ configurations are included in the impurity treatment, or

$$Z_f=\int_{-\infty}^{\infty}d\omega e^{-\beta\omega}\left[\rho^{(0)}(\omega)+\sum_{\nu}\rho_{\nu}^{(1)}(\omega)\right], \tag{8}$$

when only $f^0$-$f^1$ fluctuations are described in the impurity model. $\rho^{(n)}$ are the spectral functions for the $f^n$ configurational Green's functions, i.e.,

$$\rho^{(0)}(\omega)=\frac{1}{\pi}\mathrm{Im}\,G^{(0)}(\omega),$$

$$\rho_{\nu}^{(1)}(\omega)=\frac{1}{\pi}\mathrm{Im}\,G_{\nu}^{(1)}(\omega), \tag{9}$$

$$\rho_{\nu\nu'}^{(2)}(\omega)=\frac{1}{\pi}\mathrm{Im}\,G_{\nu\nu'}^{(2)}(\omega),$$

with

$$G^{(0)}(\omega)=\sum_{N_c}\frac{e^{-\beta E_{N_c}}}{Z_c}\left\langle N_c\left|\frac{1}{\omega-\hat{H}_{N_c}}\right|N_c\right\rangle,$$

$$G_{\nu}^{(1)}(\omega)=\sum_{N_c}\frac{e^{-\beta E_{N_c}}}{Z_c}\left\langle \nu;N_c\left|\frac{1}{\omega-\hat{H}_{N_c}}\right|N_c;\nu\right\rangle, \tag{10}$$

$$G_{\nu\nu'}^{(2)}(\omega)=\sum_{N_c}\frac{e^{-\beta E_{N_c}}}{Z_c}\left\langle \nu\nu';N_c\left|\frac{1}{\omega-\hat{H}_{N_c}}\right|N_c;\nu\nu'\right\rangle.$$

Here, $N_c$ is a composite index enumerating the conduction-electron states according to

$$|N_c\rangle=\hat{c}_{\nu_1\varepsilon_1}^{\dagger}\ldots\hat{c}_{\nu_N\varepsilon_N}^{\dagger}|\mathrm{vac}\rangle,$$

$$|N_c;\nu\rangle=\hat{c}_{\nu_1\varepsilon_1}^{\dagger}\ldots\hat{c}_{\nu_N\varepsilon_N}^{\dagger}\hat{f}_{\nu}^{\dagger}|\mathrm{vac}\rangle, \tag{11}$$

$$|N_c;\nu\nu'\rangle=\hat{c}_{\nu_1\varepsilon_1}^{\dagger}\ldots\hat{c}_{\nu_N\varepsilon_N}^{\dagger}\hat{f}_{\nu}^{\dagger}\hat{f}_{\nu'}^{\dagger}|\mathrm{vac}\rangle,$$

where we have introduced the convenient linear combination of band states:

$$\hat{c}_{\nu\varepsilon}=\frac{1}{\sqrt{|V_{\nu}(\varepsilon)|^2}}\sum_{n\mathbf{k}}V_{\nu}^{n\mathbf{k}}\hat{c}_{n\mathbf{k}}\delta(\varepsilon-\varepsilon_{n\mathbf{k}}). \tag{12}$$

The normalizing prefactor is defined in Eq. (20) below. The quantities entering in Eqs. (10) are

$$E_{N_c}=\sum_{m\in N_c}\varepsilon_m, \tag{13}$$

$$\hat{H}_{N_c}=\hat{H}-E_{N_c}, \tag{14}$$

$$Z_c=\sum_{N_c}e^{-\beta E_{N_c}}. \tag{15}$$

In the generalized NCA the configurational Green's functions are given self-consistently in terms of their self-energies as

$$G^{(n)}(\omega)=\frac{1}{[G_0^{(n)}(\omega)]^{-1}-\Sigma^{(n)}(\omega)}, \tag{16}$$

where $G_0^{(n)}$ are the unperturbed Green's functions, and

$$\Sigma^{(0)}(\omega)=\sum_{\nu}\int_{-\infty}^{\infty}d\varepsilon f(\varepsilon)|V_{\nu}(\varepsilon)|^2G_{\nu}^{(1)}(\omega+\varepsilon), \tag{17}$$

$$\Sigma_{\nu}^{(1)}(\omega)=\int_{-\infty}^{\infty}d\varepsilon f(-\varepsilon)|V_{\nu}(\varepsilon)|^2G^{(0)}(\omega-\varepsilon)+\sum_{\nu'\neq\nu}\int_{-\infty}^{\infty}d\varepsilon f(\varepsilon)|V_{\nu'}(\varepsilon)|^2G_{\nu\nu'}^{(2)}(\omega+\varepsilon), \tag{18}$$

$$\Sigma_{\nu\nu'}^{(2)}(\omega)=\int_{-\infty}^{\infty}d\varepsilon f(-\varepsilon)\{|V_{\nu}(\varepsilon)|^2G_{\nu'}^{(1)}(\omega-\varepsilon)+|V_{\nu'}(\varepsilon)|^2G_{\nu}^{(1)}(\omega-\varepsilon)\}. \tag{19}$$

Here, the energy-resolved hybridization function is introduced according to

$$|V_{\nu}(\varepsilon)|^2=\sum_{n\mathbf{k}}|V_{\nu}^{n\mathbf{k}}|^2\delta(\varepsilon-\varepsilon_{n\mathbf{k}}). \tag{20}$$

When only $f^0$ and $f^1$ configurations are included, the spectral functions $\rho^{(0)}$ and $\rho^{(1)}$ are calculated in the usual NCA (Ref. 29) (generalized to more than one irreducible representation), which corresponds to the above equations (17) and (18) with the second term omitted on the right-hand side of Eq. (18). In the present context, this should not be understood as a $U\rightarrow\infty$ approximation, but rather as an assumption that the coupling to higher configurations is included in the first term $E_0$ of Eq. (3). This will be discussed in greater detail below. For the case where the $f^2$ configurations are also included in the impurity calculation, we have included vertex correction terms to the self-energies in Eqs. (17)–(19), as discussed in Refs. 30 and 31.

Having found the Helmholtz free energy of the system, the pressure-volume curve may be calculated from the relation

$$p(T,v)=-\frac{\partial F(T,v)}{\partial v}. \tag{21}$$

If the $pv$ curve is not monotonous, i.e., if two volumes can exist at a given pressure, the stable volume will be the one minimizing the Gibbs free energy

$$G(T,p)=F[T,v(T,p)]+pv(T,p) \tag{22}$$

To summarize, the philosophy behind the present treatment of the $\alpha$-$\gamma$ transition in Ce is similar to that of the KVC

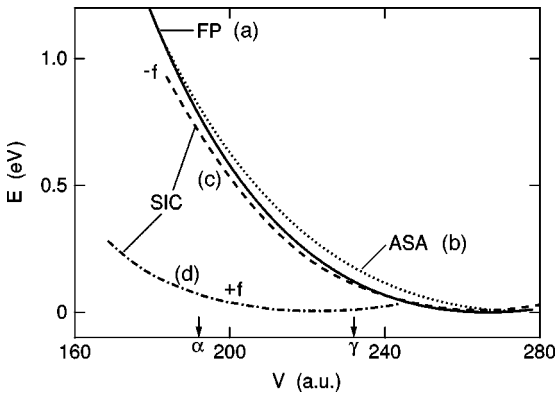


FIG. 1. Total-energy curves for Ce calculated by different DFT methods. The curves have been shifted by constant energy offsets to facilitate comparison. (a) Full curve: FP LDA calculation, (b) dotted curve: LDA calculation with the ASA, (c) dashed and (d) dash-dotted curves: SIC-LDA calculations with the ASA. In (d), the $f$ hybridization was included for the conduction states, but not in (a), (b), and (c). The arrows mark the experimental volumes of the $\alpha$ and $\gamma$ phases (192 a.u. and 232 a.u., respectively.)

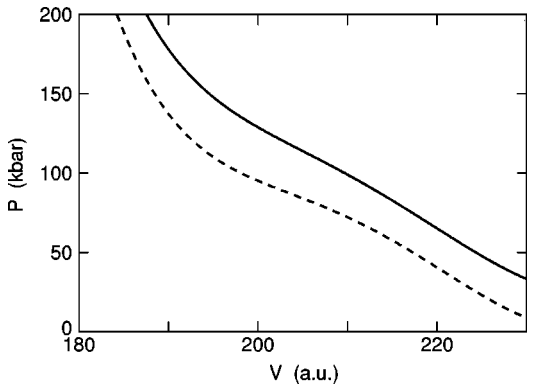


FIG. 2. Pressure-volume curves for Ce calculated from the sum of FP-LDA energies, excluding $f$ hybridization, and full extended NCA free energies from the Anderson impurity model. The solid curve shows results with the same hybridization strength for all configuration interactions, while the dashed curve is calculated with $f^1$-$f^2$ hybridization increased by a factor of 2.

model described by Allen and Liu.[14] The difference between the two calculations is in the technical details: Here, total energy curves are calculated from *ab initio* band-structure schemes instead of the empirical curve used in Ref. 14 for estimating the total energy in the absence of $f$-$spd$ hybridization. In addition we use the NCA scheme and its extensions to perform a direct calculation of the Helmholtz free energy.

## IV. NUMERICAL RESULTS AND DISCUSSION

### A. Impurity-model treatment of multiple occupancy

We shall begin by considering the case of a DFT calculation without any $f$ contribution to the cohesion in conjunction with an impurity-model calculation including $f^0$, $f^1$, and $f^2$ configurations. The DFT calculation in question can be realized either by treating the $4f$ orbitals as a partially filled core shell, or by doing a SIC calculation in which the normal conduction states are not expanded in $4f$ orbitals.

LDA calculations were performed with the $f$ states treated as core states using the LMTO method,[26] with both the atomic-spheres approximation (ASA) and the full-potential (FP) approach. In the ASA, the crystal volume is divided into overlapping atom-centered spheres with a volume equal to the actual crystal volume, and the crystal volume is assumed spherically symmetric inside the spheres. The FP method does not invoke any shape approximations for the crystal potential. The ASA is usually adequate for highly symmetric close-packed systems and has been successfully applied to Ce.[6–8] The FP calculations were done using the code developed by Wills.[32] In addition, we have performed SIC-LDA calculations with $spd$-expanded Bloch states using the ASA approximation. In all cases, a double basis set, including $5spd$ and $6sp$ orbitals, was used to ensure a correct treatment of the $5sp$ semicore states.

The total-energy curves are shown in Figs. 1(a)–1(c) (shifted to facilitate comparison). The LDA and SIC-LDA total-energy curves are quite similar showing that the ASA is quite adequate for Ce, and that the essential effect of the self-interaction correction is to turn off the *f-spd* hybridization (by shifting the *f*-level position down in energy). The position of the energy minimum is 12–18 % larger than the experimental $\gamma$-phase volume ($\sim$232 a.u.). In contrast, when the $f$ electrons are allowed to hybridize into the conduction bands in the SIC-LDA calculation the total-energy curve shown in Fig. 1(d) is obtained, with the position of the energy minimum $\sim$5% below the $\gamma$-phase volume. A similar LDA calculation including $f-spd$ hybridization found the minimum energy at $\sim$167 a.u., i.e., 13% lower than the experimental $\alpha$-phase volume (192 a.u.).[16]

In Fig. 2 the pressure-volume curve obtained by adding an impurity-model free energy to the FP-LMTO energy in Fig. 1 is shown (solid curve). The impurity model was treated by the (vertex-corrected) generalized NCA approximation described in Sec. III. The calculations were done at a temperature of 300 K with an energy axis in the range $[-1,1.5]$ Ry and a mesh spacing of 0.5 mRy. The value of the $f$ level Coulomb repulsion was set at $U=6$ eV, $\varepsilon_f$ was chosen to be $-1.27$ eV for the $j=\frac{5}{2}$ states, with a spin-orbit splitting of 0.28 eV, and the hybridization function was calculated directly from the $4f$-projected DOS, $n_\nu$, arising in the full-potential-LDA calculation:[33]

$$|V_\nu(\varepsilon)|^2=-\frac{1}{\pi}\mathrm{Im}\left[\int d\omega\frac{n_\nu(\omega)}{\varepsilon-\omega-i\delta}\right]^{-1}. \qquad (23)$$

The values for $U$ and the *f*-level positions were obtained by Liu and Allen from spectroscopic fits.[14] The steep rise of the pressure-volume curve shows that the gain of hybridization energy in the impurity model as one goes towards lower volumes cannot compensate the rise in the DFT energy curve in Fig. 1. As a result, the $\alpha$-$\gamma$ transition cannot be described within this theory, although the $pv$ curve does show a marked irregular behavior.

One can imagine at least two reasons for the discrepancy between the present model and the work of Allen and Liu. First, the LDA could be inaccurate for the computation of the energy $E_0(v)$ of the starting trivalent configuration. The LDA is known to overestimate bulk moduli, in some cases by a considerable percentage (50–100 %). This would make

the LDA total energy curve too steep, and thus favor the higher volumes in the present calculation. On the other hand, the errors in bulk moduli are usually accompanied by an underestimate of the equilibrium volume, which pulls in the other direction. Therefore, the total effect of the likely LDA errors is not obvious. A second explanation could be that we are making an error in using the same hybridization function to describe both $f^0$-$f^1$ and $f^1$-$f^2$ hopping processes. Gunnarsson and Jepsen[34] have argued that the coupling from one configuration to another should be calculated using a wave function corresponding to the configuration with the highest $f$ occupation. This means, that the $f^0$-$f^1$ coupling should be calculated with a wave function corresponding to a singly occupied state, while the $f^1$-$f^2$ coupling should be calculated using a doubly occupied orbital, which would be considerably expanded due to the internal Coulomb repulsions. Gunnarsson and Jepsen showed that this could lead to an $f^1$-$f^2$ hybridization several times larger than the one corresponding to $f^0$-$f^1$ processes. For Ce they estimated an enhancement factor of 2. The dashed curve in Fig. 2 shows the pressure-volume curve obtained if such an enhancement factor is included in the impurity-model calculations. As expected, the curve is brought down to lower pressures by the enhancement of hybridization, but, remarkably, it is still far from showing a discontinuous transition. It seems likely that both the impurity-model parameters *and* the DFT description of the ''unhybridized'' case need improvement for this approach to a modeling of the $\alpha$-$\gamma$ transition to be fruitful. Since we presently have no reliable way of estimating the precise magnitude of the rescaling factor for the $f^1$-$f^2$ hybridization, we have not gone further along this line of research. A SIC-LDA calculation assuming two localized $f$ electrons on the Ce atom is not numerically stable. It must be concluded that a treatment of the $f^1$-$f^2$ coupling within the Anderson impurity model, combined with an LDA or SIC-LDA treatment of the electron gas surrounding the $f$ multiplet, cannot be used for describing the $\alpha$-$\gamma$ transition.

### B. Density-functional treatment of multiple occupancy

In light of these findings, we now turn to the second scheme described in the previous section in which the Helmholtz free energy from an impurity-model calculation including only $f^0$ and $f^1$ configurations is added to the total energy from a SIC-LDA calculation with the Bloch states expanded in the $4f$ states orthogonal to the localized SIC state. A hybridization function is extracted from the SIC calculation using the following expression:

$$|V_\nu(\varepsilon)|^2=\sum_{n\mathbf{k}} |\langle \psi_{n\mathbf{k}}|\hat{H}_{LDA}|\psi_\nu^{SIC}\rangle|^2 \delta(\varepsilon-\varepsilon_{n\mathbf{k}}). \quad (24)$$

The states $n\mathbf{k}$ are the Bloch states, while $\nu$ indexes the possible symmetries of the SIC state. $\hat{H}_{LDA}$ is the LDA Hamiltonian for the band states. The matrix elements in Eq. (24) are equal to the off-diagonal Lagrange multipliers, which enter into the SIC-LDA minimization procedure to secure orthogonality between localized and itinerant states.[16] The resulting hybridization functions appear similar in magnitude to the ones obtained in ordinary LDA calculations by the method described in Eq. (23). By choosing SIC states of different symmetries, hybridization functions for different irreducible representations of the crystal point group can be obtained. For the cubic symmetry of the fcc lattice there are five different representations when spin-orbit splitting is included. To account for possible effects of hybridization-induced crystal-field splittings, we have performed SIC-LDA calculations with SIC states of all representations, and extracted corresponding hybridization functions. The hybridization functions are shown in Fig. 3. The total energies obtained from these SIC-LDA calculations have slight differences (mostly below 1 mRy), which could be taken to represent bare $f$-level splittings, but since the present calculations do not include electrostatic shifts, due to the symme-

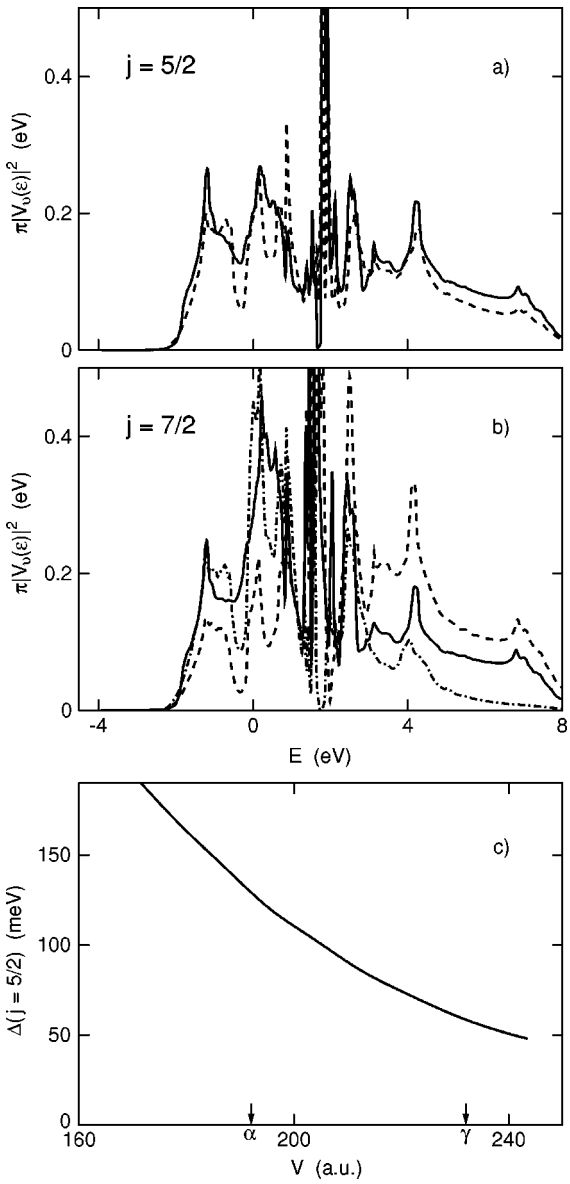


FIG. 3. The hybridization functions $\pi|V_\nu(\varepsilon)|^2$ [Eq. (24)] for (a) $j=5/2$ and (b) $j=7/2$, calculated for a Wigner-Seitz radius of 3.65 a.u.. The full, dashed, and dashed-dotted curves are for the $\Gamma_7$, $\Gamma_8$, and $\Gamma_6$ representations, respectively. The Fermi level is at $E=0$. (c) shows the volume variation of the integrated weight of $\pi|V_\nu(\varepsilon)|^2$ below the Fermi level. [Average for the $j=5/2$ multiplet and scaled by a factor $\kappa(v)=0.660-(v-199.2)/1000.6$, with $v$ in a.u.] The experimental $\alpha$ and $\gamma$ volumes are marked.

trization of the potential in the ASA, these differences are not representative of crystal-field splittings in the real system. Therefore, we have chosen to work with degenerate $f$ levels apart from the spin-orbit splitting. For the bare SIC energies [$E_0(v)$ in Eq. (3)] we have taken the energies corresponding to the $\Gamma_7$ representation of the $j=\frac{5}{2}$ multiplet. Figure 1(d) shows the calculated total energy when the conduction states are allowed to hybridize with the $f$ states. The bare $f$-level energies were the same as in the calculations described in the previous subsection.

The strength of the hybridization function, and the variation of this strength with volume, has a decisive influence on the thermodynamics of the system, but the procedure of calculating this function within the LDA or SIC-LDA is fairly crude and does not capture several important aspects of the system. For instance, a hybridization function, which is calculated including lattice effects, as realizable within the dynamical mean-field theory (DMFT),[35] might evolve $f$-related structures at the Fermi level,[31] which could considerably influence the free energy. Also dynamical correlations among the $d$ electrons could modify the LDA hybridization functions,[14,36] as could correlation-induced changes in the $f$-occupation number. Since we cannot at present treat all these problems, we must instead modify our hybridization functions to conform to experimental information, as was also done by Liu and Allen. These authors gave values for the average of the hybridization strengths in a 3-eV region below the Fermi level at the $\alpha$- and $\gamma$-phase volumes. In this work, we have chosen rescaling factors for each of these volumes so that the average of the hybridization strengths for the $j=\frac{5}{2}$ representations obtained from our calculations agree with the ones quoted by Liu and Allen after rescaling. For the other volumes, the rescaling factor was assumed to vary linearly with volume. The necessary scaling factors are 0.660 in the $\alpha$ phase and 0.626 in the $\gamma$ phase, somewhat smaller than the factors used by Liu and Allen, due to the different procedures for calculating the hybridization. Figure 3(c) shows the volume dependence of the averaged hybridization strength, defined as

$$\Delta=\pi\frac{1}{6}\sum_{\nu}^{(j=5/2)}\frac{1}{\varepsilon_F-B}\int_B^{\varepsilon_F}|V_\nu(\varepsilon)|^2 d\varepsilon, \tag{25}$$

where $B$ defines the bottom of the conduction bands. This quantity indeed varies close to linearly with volume. In summary, we have used the (experimentally fitted) information obtained by Liu and Allen to obtain the bare $f$-level positions and the average hybridization strengths, whereas no other adjustable parameters enter in the calculation.

In Fig. 4 the pressure-volume isotherms obtained from the KVC calculation are shown. The dotted lines indicate the positions of the phase transition, as found by requiring the Gibbs free energy to be minimized. Calculations were performed at temperatures ranging from 50 K to 600 K, in steps of 50 K. The volumes of the $\alpha$ and $\gamma$ phases lie in the ranges 180–185 a.u. and 205–210 a.u., respectively, at the transition pressure. At room temperature (300 K) the volumes are 182 a.u. and 205 a.u. In comparison, the experimental $\alpha$ volumes at this temperature are around 185–190 a.u.,[1,37] while the $\gamma$ volume at the transition pressure has been found to be $\sim$215 a.u.[37] Thus, the errors in the description of these

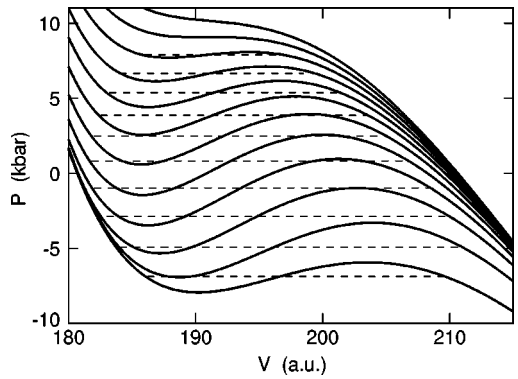


FIG. 4. Isothermal pressure-volume curves calculated in the present version of the KVC model. Total energies are calculated with the SIC-LDA including $f$ hybridization and free energies are obtained from the NCA treatment of the Anderson impurity model. Dashed lines mark the $\alpha$-$\gamma$ transition. Isotherms are for $T=n\times 50$ K, $n=1,2,\ldots,12$.

volumes are less than $\sim$5%, which is quite common in LDA calculations for ''normal'' solids. At zero pressure, the results are less satisfactory: The $\gamma$ phase in this case has an equilibrium volume of 232 a.u.,[1] compared to the $\sim$210 a.u. found from the curve in Fig. 4. This shows that we are overestimating the bulk modulus of the $\gamma$ phase at low pressures. For the $\alpha$ phase, at $T=77$ K, theoretical and experimental results are $\sim$181 a.u. and 192 a.u.,[1] respectively.

In Fig. 5 the $pT$ phase diagram calculated from the curves in Fig. 4 is shown (dashed curve), together with the experimental phase transition line (solid line). The latter has been extrapolated into the region below 200 K, where a third phase of Ce, the hexagonal $\beta$ phase, is actually reached. It is seen that the slopes of the curves are quite similar, but the theoretical curve appears at somewhat lower pressures, indicating that our model is favoring the $\alpha$ phase too much. The upper critical point in the calculation appears at 550 K, in accordance with the experimental value of $600\pm 50$ K. A slight curvature towards the temperature axis has been reported in some experiments,[1] though not all, and is also seen in the theoretical curve, but has not been included in the experimental phase boundary. We have extended both curves to the lowest temperature reached in our calculations (50 K), but do not intend to indicate the presence of a lower critical

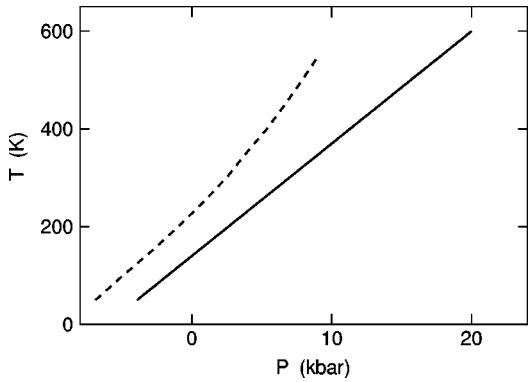


FIG. 5. Theoretical and experimental $p$-$T$ phase transition line for the $\alpha$-$\gamma$ transition. The solid curve shows the experimental line, while the dashed curve shows theoretical results.

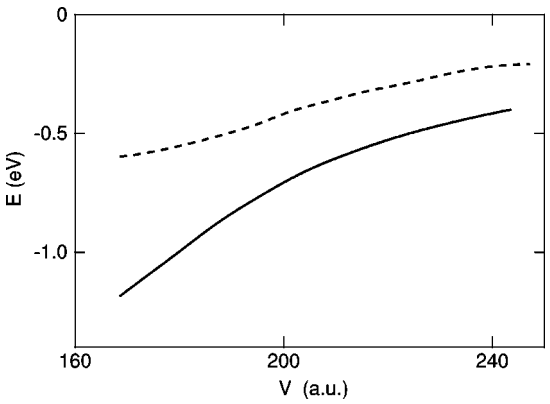


FIG. 6. Comparison of $f^1$-$f^2$ hybridization energy as calculated with the Anderson impurity model in the NCA (dashed line) and by the SIC-LDA method (solid line). See text for explanation.

point at this value. The existence of such a point (at negative pressure and a temperature below 40 K) was predicted by the KVC calculation of Allen and Liu. Alloying experiments, which mimic negative pressures by expanding the Ce lattice, have provided some support for this finding.[38] From the curves in Fig. 4 it seems dubious that such a point would appear in the present calculation, but its existence cannot be excluded since our numerical calculations become unreliable at very low temperatures. The critical volume is calculated to be $V_c = 192$ a.u., approximately 5% smaller than the experimental value of 202 a.u.[39] In connection with the phase boundary it should be noted that the product of transition pressure and volume change is typically on the order of $p\Delta v \sim 0.1$–$1$ mRy, which means that the position of the phase boundary is quite sensitive to changes in, e.g., the shape of the SIC-LDA total energy curve on this energy scale. In fact, the difference between theory and experiment seen in Fig. 5 could easily be caused by errors of the kind usually found in LDA calculations for weakly correlated materials. The transition volumes are a more ''robust'' quantity to calculate, and it is therefore reassuring to see that they come out with only small to moderate errors.

In total, the model presented here for the $\alpha$-$\gamma$ transition in Ce has comparable, or better, agreement with experimental results than any other calculation put forward so far. In particular, the tendency of models based purely on DFT to produce too large volume collapses and critical-point temperatures (e.g., 23% at room temperature and $T_c = 1300$ K in the calculation of Svane[16]) has been cured by inclusion of impurity-model-based $f^0$-$f^1$ hybridization energies. The volume collapse at room temperature is predicted to be 11.3% in the present work, and 8.8% in the calculation of Allen and Liu, while the experimental value is 14.8%.[1] In the work of Allen and Liu, the $\alpha$ and $\gamma$ volumes both appear too high, while in the work of Svane, the $\gamma$ volume is predicted quite accurately at the transition pressure, while the $\alpha$ volume is severely underestimated. In the present work, both volumes are predicted with fair accuracy.

To investigate the difference between the two types of calculations discussed here we show in Fig. 6 the $f^1$-$f^2$ contribution to $F\ (T=0\ \mathrm{K}, v)$. In approach A, this quantity is calculated as the difference in free energy of the Anderson impurity model using the extended NCA and the strict NCA. In approach B it is given as the difference between the SIC-LDA total energies with and without $f$-state hybridization in the conduction bands [curves (d) and (c) in Fig. 1]. It is seen that the $f^1$-$f^2$ hybridization energy is about twice as large in approach B as in approach A. Since approach B leads to the correct description of the phase transition we are led to conclude that the $f^1$-$f^2$ contribution to the total energy is inadequately described by the extended NCA, even when including vertex corrections.

Although the present model provides good quantitative results, it should be recognized that it contains several unclear points. To interpret the calculation in impurity-model language we must imagine that the NCA calculation describes fluctuations between the $f^0$ configuration and a set of states that we call $f^1$ states, but which are in reality mixtures of $f^1$ and higher configurations. If that is the case, it is not clear how the hybridization between such states should be calculated. This may be less important, since we end up rescaling the hybridization strength according to experimental fits. However, these fits were done using calculations within the Gunnarsson-Schönhammer formalism, and, more importantly, they were done using the same hybridization function for all configurational interactions. As we have seen, it is likely that the $f^1$-$f^2$ hybridization needs to be rescaled, and one could then question the fits of Liu and Allen.

A point where the impurity-model picture is clearly at variance with SIC-LDA and LDA is the question of the $f$-occupation number. In the SIC-LDA calculation the occupation of the $4f$ orbital is around 1.3 electrons in both the $\alpha$ and the $\gamma$ phase, while the impurity model always predicts an occupation around 1, or lower, even when the $f^1$-$f^2$ hybridization function is rescaled by a factor of 2. One can argue that the occupation number of the Kohn-Sham orbitals in DFT is not necessarily physically relevant. On the other hand, the total charge distribution should be a physical quantity (if we believe in the SIC-LDA), and the $4f$ orbital is spatially well separated from the rest of the valence orbitals.

To make progress from this somewhat unsatisfactory situation, one would probably need a better understanding of the hybridization function. First of all, one should seek a method for estimating configuration-dependent hybridization strengths as advocated by Gunnarsson and Jepsen, and second, due to the sensitivity of the calculation to the hybridization strength near the Fermi level, lattice effects (i.e., the effect of DMFT self-consistency) and possibly effects of correlations among the Ce $d$ electrons not captured by LDA may be important. Finally, the total-energy calculations without inclusion of $f$ hybridization could be improved by using, e.g, the GGA (Ref. 23) instead of the LDA.

## V. CONCLUSIONS

We have investigated two possible ways of describing the $\alpha$-$\gamma$ transition in Ce by a combination of parameter-free DFT electronic structure calculations and Anderson impurity-model calculations. In the first approach the hybridization between the $f$ electrons and the surrounding electron gas is described entirely by the impurity model, treating the $4f$ multiplet as a singly occupied core state in the DFT calculation, and including all possible states (in practice restricted to $f^0$, $f^1$, and $f^2$ states) in the many-body treatment

of the impurity model. In the second approach the coupling between $f^1$ and higher configurations is described by DFT in the SIC-LDA, while only the coupling between $f^0$ and $f^1$ configurations is treated by means of the impurity model. The first method seems incapable of describing the transition with parameters chosen according to present knowledge, whereas the second method gives a fairly accurate quantitative account for the phase diagram, but is more difficult to interpret because the $f^1$ configuration as represented by the SIC-LDA calculation is in fact a dressed $f^1$ configuration. We conclude that the mapping of the parameter-free electronic structure calculations to model Hamiltonians like the Anderson impurity model is best understood as an effective mapping. A better understanding of the hybridization function entering the impurity model, as well as a better way of describing the unhybridized case by DFT, will be needed for a full understanding of the phenomenon. Finally, the effects of the lattice need to be addressed.

## ACKNOWLEDGMENTS

Discussions with Professor J. W. Allen, who encouraged us to look into the KVC model using DFT, are gratefully acknowledged.

[1] D. C. Koskenmaki and K. A. Gschneider, in *Handbook on the Physics and Chemistry of Rare Earths*, edited by K. A. Gschneider and L. Eyring (North-Holland, Amsterdam, 1978), Chap. 4.
[2] B. Coqblin and A. Blandin, Adv. Phys. **17**, 281 (1968); R. Ramirez and L. M. Falicov, Phys. Rev. B **3**, 1225 (1971).
[3] B. Johansson, Philos. Mag. **30**, 469 (1974).
[4] D. R. Gustafsson, J. D. McNutt, and L. O. Roellig, Phys. Rev. **183**, 435 (1969).
[5] D. M. Wieliczka, C. G. Olson, and D. W. Lynch, Phys. Rev. B **29**, 3028 (1984); F. Patthey, B. Delley, W.-D. Schneider, and Y. Baer, Phys. Rev. Lett. **55**, 1518 (1985).
[6] D. Glötzel, J. Phys. F **8**, L163 (1978); D. Glötzel and R. Podloucky, Physica (Amsterdam) **102B&C**, 348 (1980).
[7] W. E. Pickett, A. J. Freeman, and D. D. Koelling, Phys. Rev. B **23**, 1266 (1981).
[8] B. I. Min, H. J. F. Jansen, T. Oguchi, and A. J. Freeman, Phys. Rev. B **34**, 369 (1986).
[9] J. M. Wills, O. Eriksson, and A. M. Boring, Phys. Rev. Lett. **67**, 2215 (1991); O. Eriksson, J. M. Wills, and A. M. Boring, Phys. Rev. B **46**, 12 981 (1992).
[10] J. Hubbard, Proc. R. Soc. London, Ser. A **276**, 238 (1963); **277**, 237 (1964); **281**, 401 (1964).
[11] P. W. Anderson, Phys. Rev. **124**, 41 (1961).
[12] J. W. Allen and R. M. Martin, Phys. Rev. Lett. **49**, 1106 (1982); R. M. Martin and J. W. Allen, J. Magn. Magn. Mater. **47&48**, 257 (1985).
[13] M. Lavagna, C. Lacroix, and M. Cyrot, Phys. Lett. **90A**, 210 (1982); J. Phys. F **13A**, 1007 (1983).
[14] L. Z. Liu, J. W. Allen, O. Gunnarsson, N. E. Christensen, and O. K. Andersen, Phys. Rev. B **45**, 8934 (1992); J. W. Allen and L. Z. Liu, *ibid.* **46**, 5047 (1992).
[15] B. Johansson, I. A. Abrikosov, M. Aldén, A. V. Ruban, and H. L. Skriver, Phys. Rev. Lett. **74**, 2335 (1995).
[16] A. Svane, Phys. Rev. B **53**, 4275 (1996).
[17] T. Jarlborg, E. G. Moroni, and G. Grimvall, Phys. Rev. B **55**, 1288 (1997).
[18] J. P. Perdew and A. Zunger, Phys. Rev. B **23**, 5048 (1981).
[19] R. O. Jones and O. Gunnarsson, Rev. Mod. Phys. **61**, 689 (1989).
[20] J. Kübler and V. Eyert, in *Electronic Structure Calculations*, Vol. 3a of *Materials Science and Technology*, edited by R. W. Cahn, P. Haasen, and E. J. Kramer (Weinheim, New York, 1993), p. 1.
[21] O. Gunnarsson and K. Schönhammer, Phys. Rev. B **28**, 4315 (1983); **31**, 4815 (1985).
[22] Including vibrational free energy, as in Ref. 17, reduces the critical point coordinates to $(p_c, T_c) = (40$ kbar, 1150 K); A. Svane (unpublished).
[23] D. C. Langreth and M. J. Mehl, Phys. Rev. B **28**, 1809 (1983); J. P. Perdew and Y. Wang, *ibid.* **33**, 8800 (1986); J. P. Perdew, *ibid.* **33**, 8822 (1986).
[24] P. Söderlind, O. Eriksson, B. Johansson, and J. M. Wills, Phys. Rev. B **50**, 7291 (1994).
[25] A. Svane, Phys. Rev. B **51**, 7924 (1995).
[26] O. K. Andersen, Phys. Rev. B **12**, 3060 (1975).
[27] O. K. Andersen and O. Jepsen, Phys. Rev. Lett. **53**, 2571 (1984).
[28] O. K. Andersen, O. Jepsen, and O. Glötzel, in *Canonical Description of the Band Structures of Metals*, Proceedings of the International School of Physics, Course LXXXIX, Varenna, 1985, edited by F. Bassani, F. Fumi, and M. P. Tosi (North-Holland, Amsterdam, 1985), p. 59.
[29] N. E. Bickers, D. L. Cox, and J. W. Wilkins, Phys. Rev. B **36**, 2036 (1986).
[30] T. Pruschke and N. Grewe, Z. Phys. B **74**, 439 (1989).
[31] J. Lægsgaard and A. Svane, Phys. Rev. B **58**, 12 817 (1998).
[32] J. M. Wills (unpublished); J. M. Wills and B. R. Cooper, Phys. Rev. B **36**, 3809 (1987); D. L. Price and B. R. Cooper, *ibid.* **39**, 4945 (1989).
[33] O. Gunnarsson, O. K. Andersen, O. Jepsen, and J. Zaanen, Phys. Rev. B **39**, 1708 (1989).
[34] O. Gunnarsson and O. Jepsen, Phys. Rev. B **38**, 3568 (1988).
[35] A. Georges, G. Kotliar, W. Kraut, and M. J. Rozenberg, Rev. Mod. Phys. **68**, 13 (1996); and references therein.
[36] T. Schork and S. Blawid, Phys. Rev. B **56**, 6559 (1997).
[37] W. H. Zachariasen and F. H. Ellinger, Acta Crystallogr., Sect. A: Cryst. Phys., Diffr., Theor. Gen. Crystallogr. **A33**, 155 (1977).
[38] J. D. Thompson, Z. Fisk, J. M. Lawrence, J. L. Smith, and R. M. Martin, Phys. Rev. Lett. **50**, 1081 (1983).
[39] R. I. Beecroft and C. A. Swenson, J. Phys. Chem. Solids **15**, 234 (1960).